

Supporting Information

Atomic Sulfur Formation Mechanism on 3-Mercaptopropanoic Acid Derivatives Self-Assembled Monolayers: Understanding the C–S Bond Cleavage

Julio C. Azcárate,^{*,†} Natalia D. Aagaard,[†] Guillermo Zampieri,^{‡,¶} Eugenia
Zelaya,[†] and Mariano H. Fonticelli^{*,¶}

[†]*Centro Atómico Bariloche (CAB), Comisión Nacional de Energía Atómica – CONICET*

[‡]*Instituto Balseiro (IB), Universidad Nacional de Cuyo (UNCuyo), Bariloche, Argentina*

[¶]*Instituto de Investigaciones Fisicoquímica Teóricas y Aplicadas (INIFTA), Departamento
de Química, Facultad de Ciencias Exactas, Universidad Nacional de La Plata (UNLP) –
CONICET*

E-mail: jcazcarate@cab.cnea.gov.ar; mfonti@inifta.unlp.edu.ar

SAMs of dodecanethiol (SC12)

Figure S1 shows the S 2p region XP spectrum of a dodecanethiol-SAM on preferentially oriented Au(111) substrate. The main peak –S 2p_{3/2} at 162 eV– is attributed to adsorbed thiolate (S2). The weak and broad peak whit S 2p_{3/2} at 163.4 eV is attributed either physisorbed thiols or disulfide molecules originated by radiation damage. The S3 contribute to 3.4% of the total S 2p signal. This means that the radiation is reasonably low or not significant in our experiments.

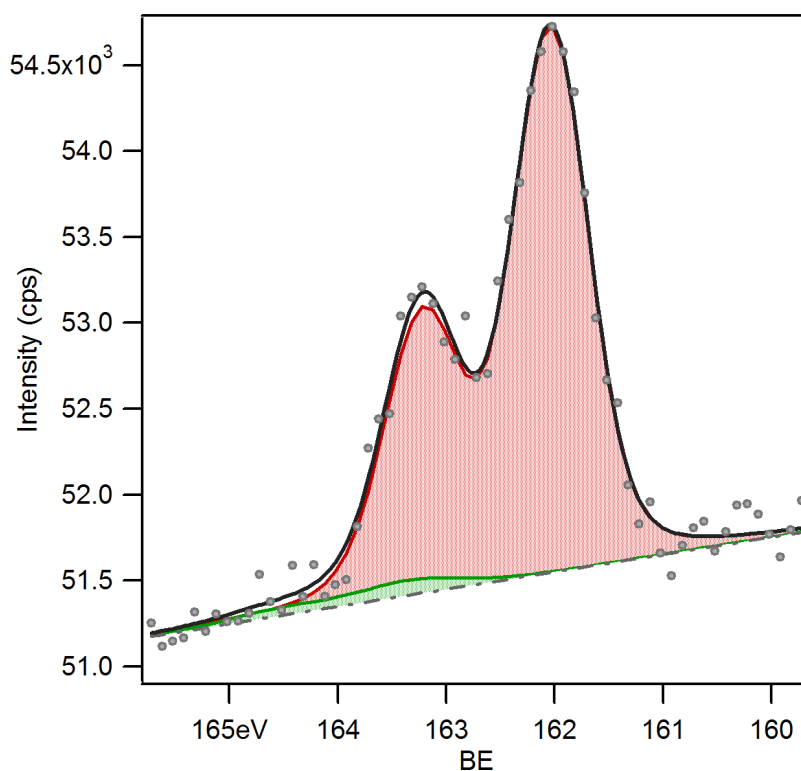
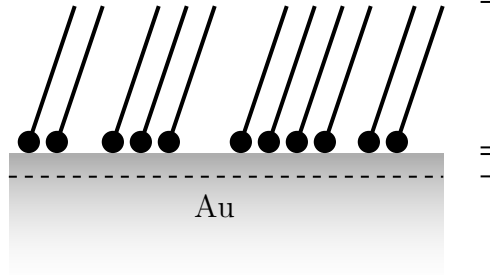


Figure S 1 – S2p region XP spectrum for SC12-SAM.: the red curve corresponds to S2 and the green curve is assigned to S3

Surface Coverage by XPS data

The surface coverage of thiol on Au is defined by:



$$\theta_S = \frac{\text{S atoms}}{\text{Au atoms on surface}} \quad (1)$$

The intensity of a XPS peak for a homogeneous solid is given by:¹

$$I_i = JK\sigma_i L_i(\gamma) \times \int_{z=0}^{\infty} N_i \exp[-z/\lambda \cos \alpha] dz \quad (2)$$

where J is the X-ray flux, K describe instrumental factors, σ_i is the photo-emission cross-section of the element i , $L_i(\gamma)$ is the asymmetry factor with γ as the angle between X-ray source and the spectrometer, N_i is the number of atoms of the elements i in a thickness z , λ is the inelastic mean free path of electrons through the solid, and α is the angle between the surface normal and the direction to the analyzer ($\alpha = 90^\circ$ in our case). The intensity due to the emission from the volumen element of thikness d , I_i^d , is related to the total intentisy I_i^∞ by the Lamber-Beer law:

$$I_i^d = I_i^\infty \left[1 - \exp\left(-\frac{d}{\lambda}\right) \right] \quad (3)$$

To estimate λ it is useful to consider the *effective attenuation lenght*, EAL.² According to Cumpson and Seah,³ the EAL for an element of atomic number z results::

$$\text{EAL [nm]} = 0.316a^{3/2} \left\{ \frac{E_K}{Z^{0.45}[\ln(E_K/27) + 3]} + 4 \right\} \quad (4)$$

where E_K is the kinetic energy of the electrons and a is the mean lattice parameter (in nm)

$$a = 10^8 \left(\frac{A_w}{\rho N_{Av}} \right)^{1/3} \quad (5)$$

In the last relation A_w is the atomic weight (in g), ρ is the density and N_{Av} the Avogadro's number. In order to express the EAL as the equivalent number of monolayer, the equation 4 can be divided by equation 5. For organic materials:^{4,5}

$$\text{EAL}_{\text{Org.Mat.}}[\text{nm}] = \frac{31}{(E_K)^2} + 0.087\sqrt{E_K}; \quad E_K < 100\text{eV} \quad (6)$$

$$\text{EAL}_{\text{Org.Mat.}}[\text{nm}] = 0,00837 \times (E_K)^{0,842}; \quad E_K > 100\text{eV} \quad (7)$$

The XPS intensity due to the Au atoms on the outer surface layer is expressed according:

$$I_{Au}^{1ML} = I_{Au}^{\infty} \left[1 - \exp \left(-\frac{1}{\lambda_{Au}} \right) \right] = JK\sigma_{Au}L_{Au}AN_{Au}^{1ML} \quad (8)$$

where A is the sampled area and N_{Au} is the number of Au atoms on surface. However, the total intensity I_{Au}^{∞} is attenuated by the organic layer of thicknes l deposited on the Au surface. Then, the meassured intensity, I_{Au}^m , is:

$$I_{Au}^m = I_{Au}^{\infty} \exp \left(-\frac{l}{\lambda_{Org}(E_{K,Au})} \right) \quad (9)$$

For a thiol monolayer, the intensty of S is given by:

$$I_S = JK\sigma_S L_S A N_S \quad (10)$$

and the signal of the S atom is attenuated by the organic layer (the hydrocarbon chains of the thiols) over it:

$$I_S^m = I_S \exp \left(-\frac{l}{\lambda_{Org}(E_{K,S})} \right) \quad (11)$$

Finally, the surface coverage of S on Au can be calculated the equation:

$$\theta_S = \frac{N_S}{N_{Au}} = \frac{I_S^m}{I_{Au}^m} \frac{\sigma_{Au} L_{Au}}{\sigma_S L_S} \frac{\exp(-l/\lambda_{Org}(E_{Au}))}{\exp(-l/\lambda_{Org}(E_S))[1 - \exp(-1/\lambda_{Au})]} \quad (12)$$

This equation can be simplified introducing some approximations. In our case $\gamma = 54.7^\circ$, then $L_i = 1$. For Al K_α X-ray source ($h\nu = 1486.6$ eV) the kinetic energy of S 2p and Au 4f electrons are rather close. Then, the attenuation experienced by S 2p and Au 4f are very similar. Then, the equation 12 can be expressed as:

$$\theta_S = \frac{N_S}{N_{Au}} \approx \frac{I_S^m}{I_{Au}^m} \frac{\sigma_{Au}}{\sigma_S} \frac{1}{[1 - \exp(-1/\lambda_{Au})]} \quad (13)$$

Finally, in table S 1 we provide the values of the constants sigma, lambda, etc. used to estimate the θ_S . The measured intensities I_i^m for each component is the area under the fitted curve after baseline subtraction.

Table S 1 – Parameters used for coverage calculation with an Al K_α X-Ray source

| Element | σ^a (Mbarn) | λ_{Au} (# of monolayers) |
|---------|--------------------|----------------------------------|
| S | 0.02265 | — |
| Au | 0.2511 | 5.15 ^b |

^a - <https://vuo.elettra.eu/services/elements/WebElements.html>
^b - calculated from equation 4

XP spectra of Au, C and O

The broad XP spectrum (survey) show all the signals present. No other elements than Au, S, C and O were found. No Hg contamination is found.

The spectra for O 1s and C 1s are the expected for a sample prepared *ex-situ*. For MPA we expect the presence of three components in the C 1s XPS spectrum: one for every kind of carbon in the adsorbed molecules. Although the large widths of the peaks do not allow for an unambiguous fitting of the spectrum, we can tentatively assign the features

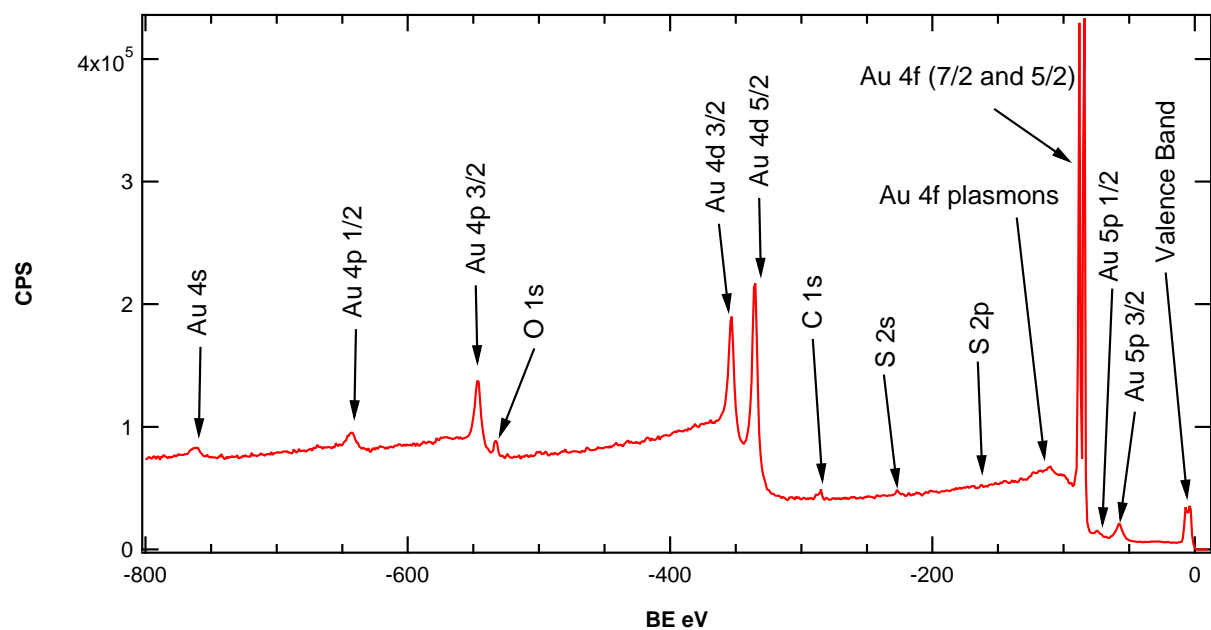


Figure S 2 – Survey spectra for Me-MPA self-assembled monolayer on Au.

in the spectrum following previous reports.⁶ First, the higher binding energy peak (broad peak around 288.5 eV) was associated to the carboxylic acid function ($-\text{COOH}$). Second, the most intense signal (centered at 284.8 eV) has contributions from the methylene carbon ($-\text{CH}_2-$) and adventitious carbon. Lastly, the poorly resolved peak at 286.5 eV is due to carbon of the mercapto group (CH_2-S). On the other hand, the carbon signal in the XPS spectrum (C 1s) of Me-MPA has at least four components, which cannot be precisely resolved do to the low separation among some of them. However, we can associate some of the peaks in the C1s region with the different carbon environments. The higher BE peak corresponds to the ester carbonyl (288.6 eV),⁷⁻⁹ while the spike centered at 286.5 eV would present contributions from the carbon singly bound to one oxygen (ester function, CH_3-O) and the carbon of the mercapto group ($-\text{CH}_2-\text{S}$). Lastly, the most intense peak has contributions from the methylene carbon ($-\text{CH}_2-$) and adventitious carbon.

The O 1s spectrum of MPA shows a broad peak that is probably composed of at least two components. The dominating low binding energy component observed at 531.42 eV is assigned to both the carbonyl oxygen ($\text{C}=\text{O}$) of the carboxylic acid function and the

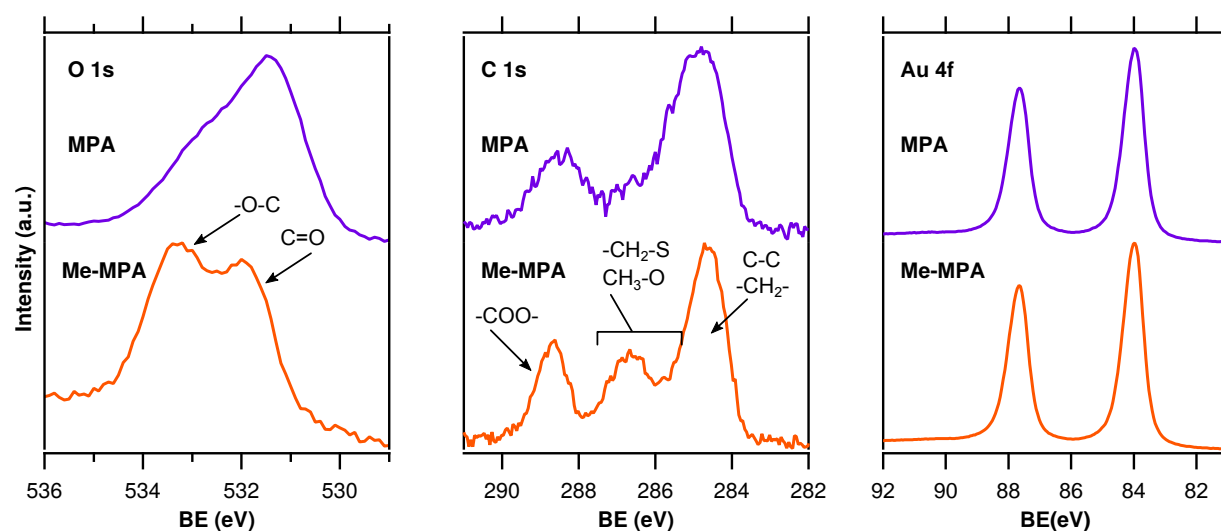


Figure S 3 – Comparison of XP spectra of O 1s, C 1s and Au 4f for MPA and Me-MPA

deprotonated carboxyl group (COO^-).¹⁰ Meantime, the shoulder at about 532.8 eV is due to the non-deprotonated carboxyl oxygen ($-\text{OH}$). However, the asymmetry on the higher BE side could also be related to the contribution of some coadsorbed water⁶ or ethanol molecules. On the other hand, for Me-MPA, the contributions of two kinds of non-equivalent oxygen can be clearly distinguished in the O 1s region. Indeed, the peak at 531.8 eV can be assigned to the carbonyl oxygen ($\text{C}=\text{O}$), while the higher binding energy one (533.2 eV) to the carboxyl oxygen (O bonded to the methyl group).⁸

Finally, the Au 4f region for both MPA and MPA SAMs presents spectra that are typical of alkanethiol SAMs.¹¹ The salient features are: (i) Au $4f_{7/2}$ components located 84.0 eV and FWHMs about 0.7 eV. Both figures are coincident with those found for dodecanethiol SAMs within the experimental error.

Electrochemical data of SAMs treated in NaOH

The Figure S4 demonstrates the strong effect of NaOH on the integrity and composition of Me-MPA SAMs. The orange-dashed line shows the data for a Me-MPA SAM grown in toluene. The continuous-black line show the desorption curve for a SAM exposed for 4 hours to a 0.1 M NaOH aqueous solution.

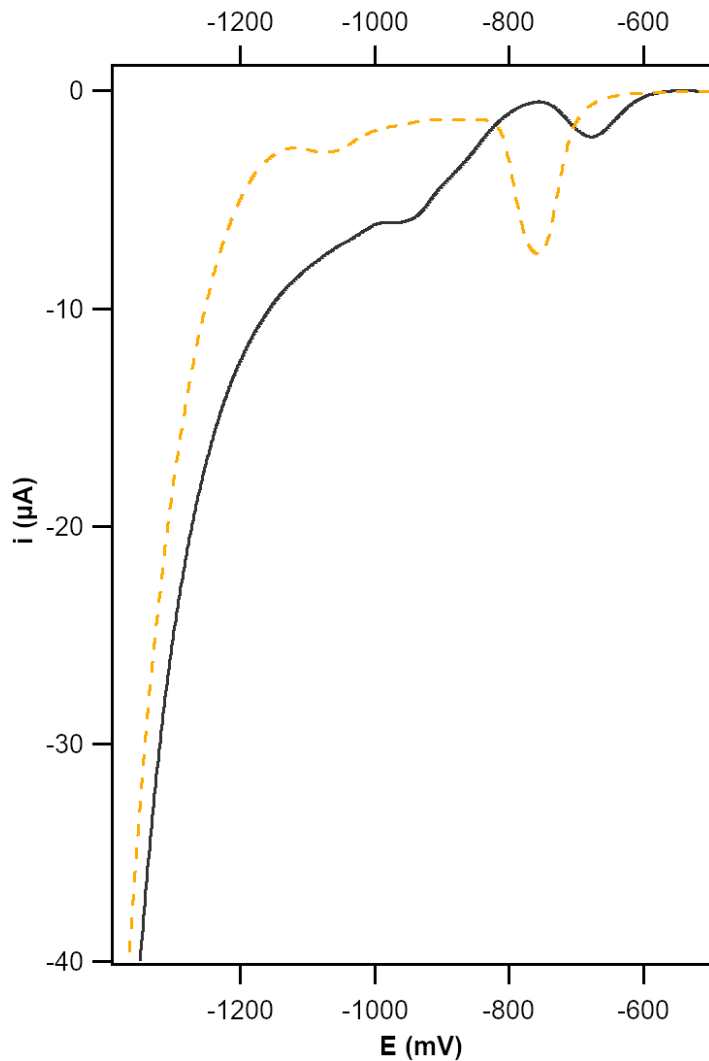


Figure S 4 – Electrodesorption curves for MeMPA SAMs. Orange-dashed line: as prepared SAM. Black-continuous line: Me-MPA SAM exposed for 4 hours to a 0.1 M NaOH aqueous solution.

References

- (1) Briggs, D.; Seah, M. P. *Practical surface analysis : by auger and x-ray photoelectron spectroscopy*; Wiley: Chichester, 1990.
- (2) Jablonski, A.; Powell, C. The electron attenuation length revisited. *Surface Science Reports* **2002**, *47*, 33–91.
- (3) Cumpson, P. J.; Seah, M. P. Elastic Scattering Corrections in AES and XPS. II. Estimating Attenuation Lengths and Conditions Required for their Valid Use in Overlay/Substrate Experiments. *Surface and Interface Analysis* **1997**, *25*, 430–446.
- (4) Seah, M. P.; Dench, W. A. Quantitative electron spectroscopy of surfaces: A standard data base for electron inelastic mean free paths in solids. *Surface and Interface Analysis* **1979**, *1*, 2–11.
- (5) Seah, M. P. Simple universal curve for the energy-dependent electron attenuation length for all materials: Simple, accurate, universal expression for attenuation lengths. *Surface and Interface Analysis* **2012**, *44*, 1353–1359.
- (6) Gonella, G.; Cavalleri, O.; Terreni, S.; Cvetko, D.; Floreano, L.; Morgante, A.; Canepa, M.; Rolandi, R. High resolution X-ray photoelectron spectroscopy of 3-mercaptopropionic acid self-assembled films. *Surface Science* **2004**, *566–568*, *P*, 638–643.
- (7) Wagner, C.; Muilenberg, G. *Handbook of X-ray Photoelectron Spectroscopy: A Reference Book of Standard Data for Use in X-ray Photoelectron Spectroscopy*; Perkin-Elmer, 1979.
- (8) Burrell, M. C.; Liu, Y. S.; Cole, H. S. An x-ray photoelectron spectroscopy study of poly(methylmethacrylate) and poly(α -methylstyrene) surfaces irradiated by excimer lasers. *Journal of Vacuum Science & Technology A* **1986**, *4*, 2459–2462.

- (9) Azcárate, J. C.; Floridia Addato, M. A.; Rubert, A.; Corthey, G.; Kürten Moreno, G. S.; Benítez, G.; Zelaya, E.; Salvarezza, R. C.; Fonticelli, M. H. Surface Chemistry of Thiomalic Acid Adsorption on Planar Gold and Gold Nanoparticles. *Langmuir* **2014**, *30*, 1820–1826.
- (10) Zubavichus, Y.; Fuchs, O.; Weinhardt, L.; Heske, C.; Umbach, E.; Denlinger, J. D.; Grunze, M. Soft X-Ray-Induced Decomposition of Amino Acids: An XPS, Mass Spectrometry, and NEXAFS Study. *Radiation Research* **2004**, *161*, 346 – 358 – 13.
- (11) Pensa, E.; Corte, E.; Fonticelli, M. H.; Benítez, G.; Rubert, A.; Salvarezza, R. C. The Chemistry of the Sulfur-Gold Interface : In Search of a Unified Model. *Acc. Chem. Res.* **2012**, *45*, 1183–1192.